

# Optimal Control of Arrays of Microcantilevers

Mariateresa Napoli<sup>1</sup> Bassam Bamieh<sup>2</sup> Mohammed Dahleh<sup>3</sup>

Department of Mechanical Engineering,  
University of California,  
Santa Barbara, CA 93106,  
U.S.A.

## Abstract

In this paper we will present a model for an array of microcantilevers that are used in Atomic Force Microscopy and nano-scale manufacturing. The microcantilevers are connected to each other through a common base, and are individually actuated. The sensors are also integrated on each microcantilever. This system is an example of a spatially-invariant system with a *distributed array of sensors and actuators*. We exploit the spatial invariance of the problem to design optimal  $\mathcal{H}_2$  controllers for this array. An analytic expression for the optimal controller is derived in the transformed domain, and estimates of the coupling range of the controller is obtained.

## 1 Introduction

For the past ten years the Atomic Force Microscope (AFM) has been developed as a tool for material imaging and characterization. The basic operation of an AFM depends on the detection and control of the deflection of a microcantilever interacting with the surface being analyzed [7, 8]. The widespread use of the AFM in applications that range from electronic to biological is a testimony to the importance of this device.

Throughput in AFM's is limited by the mechanical properties of the microcantilevers and by the detection and control design. A very important objective is to increase the throughput by improving both the design of the microcantilevers and the control system. Recently a new approach for increasing the throughput was developed where an array of microcantilevers are used to simultaneously image a surface. Control of the individual microcantilevers is achieved by a piezoelectric actuator and a piezoresistive sensor integrated on

the microcantilever [10, 11].

In this paper we study a model for an array of microcantilevers interacting with surface forces of a sample. Each microcantilever is modeled as a mass-spring system, and the interaction between a microcantilever and a sample is modeled as a Van der Waals potential. The Van der Waals potential models both the long range attractive forces as well as the short range repulsive forces. The interaction between the individual microcantilevers is modeled by a coupling matrix acting on the vector of displacements of the microcantilevers. By exploiting the spatial invariance of the problem, we design  $\mathcal{H}_2$  optimal controllers using the methodology of [4, 5, 6]. The dependence of each local controller on measurements from nearby microcantilevers is quantified by analyzing the analyticity of the optimal controllers in the transformed domain.

The paper is organized as follows: In Section 2 we develop the mathematical model of the multicantilever array and sample, in Section 3 we construct an optimal  $\mathcal{H}_2$  controller, in Section 4 we analyze the optimal controller to construct suboptimal controllers with limited sensor measurements, and finally we present our conclusions in Section 5.

## 2 Model Description

After presenting a model for a single cantilever, we show how to model an array of microcantilevers. We then show how this model fits within the general framework of *spatially invariant systems*.

### 2.1 Single Microcantilever Model

In the unimodal approximation, the cantilever-tip-sample system is modeled by a sphere of radius  $R$  and mass  $m$ , which is suspended by a spring of stiffness  $k$ . The deflection from the equilibrium position,  $Z$ , which represents the distance from the microcantilever to the sample when only the gravity is acting on it, is measured by  $x$ . The interaction with the sample is modeled

<sup>1</sup>e-mail: napoli@engineering.ucsb.edu

<sup>2</sup>e-mail: bamieh@bessel.ece.ucsb.edu. Research supported by NSF under Career award ECS-96-24152

<sup>3</sup>e-mail: dahleh@engineering.ucsb.edu. Research supported by NSF under Grant ECS-9632820, and AFOSR under Grant F49620-97-1-0168

by the Lennard-Jones potential,

$$V(x, Z) = \frac{A_1 R}{1260(Z+x)^7} - \frac{A_2 R}{6(Z+x)}, \quad (1)$$

whose two terms describe, respectively, the short range repulsive forces and the long range attractive forces between the molecules of the tip and those of the surface.  $A_1$  and  $A_2$  are the Hamacker constants for the repulsive and attractive potentials. The net energy of the system scaled by the effective mass  $m$  of the cantilever is given by

$$H(x, \dot{x}, Z) = \frac{1}{2}\dot{x}^2 + \frac{1}{2}\omega_1^2 x^2 - \frac{D\omega_1^2}{(Z+x)} + \frac{\sigma^6 D\omega_1^2}{210(Z+x)^7}, \quad (2)$$

where,  $\omega_1 = \sqrt{\frac{k}{m}}$  is the first modal frequency of the system and  $D = \frac{A_2 R}{6k}$ . Note that  $H(x, \dot{x}, Z)$ , which is the Hamiltonian of the system, is a constant of the dynamics (invariant of motion) since there is no dissipation.

Introducing the state variables  $x_1 = x$  and  $x_2 = \dot{x}$ , we can derive from (2) the equations which govern the dynamics of a single cantilever

$$\dot{x}_1 = x_2 \quad (3)$$

$$\dot{x}_2 = -\omega_1^2 x_1 - \frac{D\omega_1^2}{(Z+x_1)^2} + \frac{\sigma^6 D\omega_1^2}{30(Z+x_1)^8}. \quad (4)$$

In order to study the qualitative behavior of the system, it is convenient to perform the following change of variables. By setting  $T = \omega_1 t$ , and dividing the left and right hand sides of (3) and (4) by  $Z_s = \frac{3}{2}(2D)^{\frac{1}{8}}$ , we get

$$\xi_1' = \xi_2 \quad (5)$$

$$\xi_2' = -\xi_1 - \frac{d}{(\alpha + \xi_1)^2} + \frac{\Sigma^6 d}{30(\alpha + \xi_1)^8}, \quad (6)$$

where,  $\xi_1 = \frac{x_1}{Z_s}$ ,  $\xi_2 = \frac{x_2}{\omega_1 Z_s}$ ,  $d = \frac{4}{27}$ ,  $\alpha = \frac{Z}{Z_s}$ , and  $\Sigma = \frac{\sigma}{Z_s}$ . The prime denotes the derivative with respect to  $T$ .  $Z_s$  is the critical value of  $Z$ , below which the attractive force is greater than the spring force, and in the absence of the repulsive force the surface snaps the tip into contact, [1]. Note that the equations describing the dynamics of the dimensionalized system (3) and (4) and of the non-dimensionalized one (5) and (6) are formally the same. Hence, we can study the dynamical behavior of the former, using the equations of the latter.

As  $\alpha$  varies over  $[0, \infty]$ , the number of equilibrium points of the system varies too. In particular in [2] it is shown that there are two critical values of  $\alpha$ ,  $\alpha_{sl}$  and  $\alpha_{sv}$ . When  $\alpha < \alpha_{sv}$  there is only one equilibrium point. If  $\alpha_{sv} < \alpha < \alpha_{sl}$  the equilibrium points become three. Finally, if  $\alpha > \alpha_{sl}$  there is again only one equilibrium point.

## 2.2 Array of Microcantilevers

A multicantilever structure consists of an array of microcantilevers connected to the same beam.

Though each cantilever is actuated independently, the presence of the beam implies that its dynamics is affected by the behavior of the others. As a consequence the model we introduced for the single cantilever has to be modified to take into account this correlation. In this work we model this interaction via a symmetric infinite matrix  $a_{i,k}$ , so that the state equations for the  $i$ -th cantilever become

$$\xi_{1,i}'(t) = \xi_{2,i}(t) \quad (7)$$

$$\xi_{2,i}'(t) = -\xi_{1,i}(t) - \frac{d}{(\alpha + \xi_{1,i}(t))^2} + \quad (8)$$

$$\frac{\Sigma^6 d}{30(\alpha + \xi_{1,i}(t))^8} + \sum_{\substack{k=-\infty \\ k \neq i}}^{+\infty} a_{i,k} \xi_{1,k}(t),$$

Due to the fact that the microcantilevers are similar the coefficients  $a_{i,k}$  satisfy  $a_{i,k} = a_{i-k}$ , and decay as  $k$  goes to infinity.

Equations (7) and (8) give a local description of the system, where by local we mean limited to the  $i$ -th cantilever. In order to build a model for the whole multicantilever system, we can associate with each element a local state variable

$$\xi(i, t) = \begin{bmatrix} \xi_{1,i}(t) \\ \xi_{2,i}(t) \end{bmatrix},$$

which is a two dimensional variable, where  $i \in \mathbf{Z}$  is the spatial coordinate and  $t \in \mathbf{R}$  is the time variable. Hence the whole multicantilever will be described by a global state variable

$$\Xi(t) = \begin{bmatrix} \vdots \\ \xi(-1, t) \\ \xi(0, t) \\ \xi(1, t) \\ \vdots \end{bmatrix},$$

which is an infinite dimensional vector. Now, linearization of equations (7) and (8) around an equilibrium point leads to the following expression for the local model

$$\begin{aligned} \dot{\xi}(i, t) &= \begin{bmatrix} 0 & 1 \\ -1 + \frac{2d}{(\alpha + \xi_{1,i})^3} - \frac{4\Sigma^6 d}{15(\alpha + \xi_{1,i})^9} & 0 \end{bmatrix} \xi(i, t) + \\ &+ \sum_{j \neq i} \begin{bmatrix} 0 & 0 \\ a_{i-j} & 0 \end{bmatrix} \xi(j, t) \\ &= F\xi(i, t) + \sum_{j \neq i} B_{i-j} \xi(j, t), \end{aligned}$$

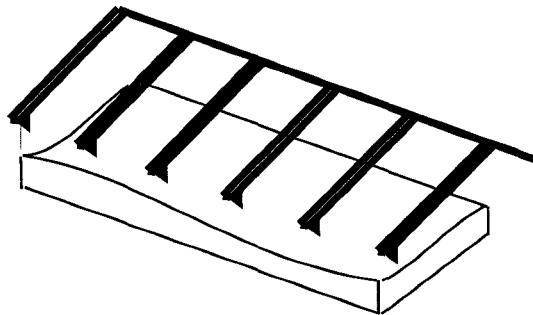


**Figure 1:** A schematic of a multicantilever structure.

so that for the whole system we have

$$\dot{\Xi}(t) = \begin{bmatrix} \ddots & & \dots & & & & & & \\ \dots & B_{-1} & F & B_1 & B_2 & & & & \\ \dots & B_{-2} & B_{-1} & F & B_1 & B_2 & \ddots & & \\ & \ddots & B_{-2} & B_{-1} & F & B_1 & \ddots & & \\ & & & \vdots & \ddots & \ddots & & & \end{bmatrix} \Xi(t) \quad (9)$$

Notice that the state matrix is block Toeplitz. As we will see, it is possible to formulate this problem in the framework of the theory of spatially-invariant distributed continuous-time systems.

### 2.3 The Microcantilever Array as a Spatially-Invariant System

Spatially-distributed continuous time systems are a particular class of multidimensional systems. From the input/output point of view, they are represented by the relationship

$$y(i, t) = \int_{-\infty}^t \left[ \sum_{j=-\infty}^{\infty} w(i-j, t-\tau) u(j, \tau) \right] d\tau, \quad (10)$$

where  $t \in \mathbf{R}$  is the time variable, and  $i \in \mathbf{Z}$  is the spatial coordinate. A system with input/output relationship (10) is causal in time, but not in space and is invariant in both time and space. This means that if  $y(i, t)$  is the output response resulting from input  $u(i, t)$ , then  $y(i-k, t-\tau)$  is the output response resulting from input  $u(i-k, t-\tau)$ .

The Fourier transform represents a convenient mathematical tool to study these systems. If we apply the Fourier transform in the spatial domain, which for a two-dimensional signal is defined as

$$S(\lambda, t) = \sum_{k=-\infty}^{\infty} s(k, t) e^{-ik\lambda},$$

we can associate the two dimensional system with a one dimensional parametric system, which is equivalent to the former, but that can be analyzed using well known

results from classical systems theory. We refer the interested reader to [3] for the main results concerning this approach in the study of spatially invariant distributed systems.

In this work we will explicitly use an important result that was shown in [5], concerning the optimal control of this class of systems. Namely, in [5] it shown that when the underlying dynamics of the system and the performance objective are spatially invariant, then optimal controllers will also have a spatial invariant structure.

The physical and, consequently, the mathematical structure of the multicantilever model allows us to embed it in the class of spatially invariant systems. This means that in order to study the multicantilever, we do not need to deal with the infinite dimensional model (9), but that we can use instead the parametrized local model.

The linearized model that we obtained earlier can be conveniently modified in the following way

$$\dot{\xi}(\cdot, t) = \begin{bmatrix} 0 & 1 \\ \mathcal{A} & 0 \end{bmatrix} \xi(\cdot, t) + \begin{bmatrix} 0 \\ 1 \end{bmatrix} u(\cdot, t), \quad (11)$$

where we have added an external input, and where  $\mathcal{A}$  is a convolution operator

$$[\mathcal{A}x(\cdot, t)](i, t) = \sum_j A_{i-j} x(j, t),$$

defined as

$$A_i = \begin{cases} -1 + \frac{2d}{(\alpha + \xi_{1,i})^3} - \frac{4\Sigma^6 d}{15(\alpha + \xi_{1,i})^9} & i = 0 \\ a_i & i \neq 0. \end{cases}$$

If we now apply the discrete Fourier transform in the spatial domain, we get the one-dimensional parametric system

$$\dot{\xi}(\lambda, t) = \begin{bmatrix} 0 & 1 \\ a(\lambda) & 0 \end{bmatrix} \xi(\lambda, t) + \begin{bmatrix} 0 \\ 1 \end{bmatrix} u(\lambda, t), \quad (12)$$

where

$$a(\lambda) = -1 + \frac{2d}{(\alpha + \xi_{1,i})^3} - \frac{4\Sigma^6 d}{15(\alpha + \xi_{1,i})^9} + \sum_{\substack{k=-\infty \\ k \neq 0}}^{\infty} a_k e^{-ik\lambda}. \quad (13)$$

### 3 $\mathcal{H}_2$ Optimal Controller

As shown in [4], once we have parameterized the distributed problem by a family of finite dimensional state space problems through the application of the Fourier transform, we can use the same results of classical finite dimensional  $\mathcal{H}_2$  theory (see [4], [3]). More precisely, after using spatial transforms, the problem can be stated as the minimization of the cost functional

$$J = \frac{1}{2\pi} \int_0^{2\pi} \int_0^\infty [\xi(\lambda, t)^* Q \xi(\lambda, t) + u(\lambda, t)^* R u(\lambda, t)] dt d\lambda$$

subject to

$$\dot{\xi}(\lambda, t) = F(\lambda)\xi(\lambda, t) + B(\lambda)u(\lambda, t),$$

with  $\xi(\lambda, 0) = \xi_0(\lambda)$ . Since the system is stabilizable, its unique solution is given by the feedback control law

$$u(\lambda, t) = -R^{-1}(\lambda)B^*(\lambda)P(\lambda)\xi(\lambda, t)$$

where  $P(\lambda)$  is the positive definite solution of the parameter-dependent algebraic Riccati equation

$$\begin{aligned} F^*(\lambda)P(\lambda) + P(\lambda)F(\lambda) + Q(\lambda) \\ - P(\lambda)B(\lambda)R^{-1}(\lambda)B^*(\lambda)P(\lambda) = 0. \end{aligned} \quad (14)$$

In our case, the state model is given by (12), and if we take

$$R = \begin{bmatrix} 1 & 0 \\ 0 & 1 \end{bmatrix} \quad Q = \begin{bmatrix} q & 0 \\ 0 & q \end{bmatrix}$$

the matrix which defines our stabilizing controller is

$$K(\lambda) = - \left[ a(\lambda) + \sqrt{a(\lambda)^2 + q} \quad \sqrt{2a(\lambda) + 2\sqrt{a(\lambda)^2 + q} + q} \right],$$

where  $a(\lambda)$  is as defined in equation (13). The fact that  $K(\lambda)$  is irrational in  $\lambda$  means that the controller needs to look at distant points to compute the control input at each given point. In real time, the feedback control law is implemented using the coefficients of a Laurent series expansion of  $K(\lambda)$  in an open annulus that contains the unit circle. If  $K(z)$  is the analytic extension of  $K(\lambda)$  in such an annulus, its Laurent power series expansion will be

$$K(z) = \sum_{h=-\infty}^{\infty} K(h)z^h, \quad (15)$$

so that the resulting optimal control law is given by

$$u(h, t) = \sum_{i=-\infty}^{\infty} K(i)\xi(h - i, t).$$

From an implementation point of view, the issue of how large is the number of state variables the controller needs to know is crucial. If the Laurent expansion coefficients of  $K(\lambda)$  decay to zero fast enough, it is reasonable to expect that a satisfactory suboptimal control law can be achieved by truncating the infinite series expansion.

### 4 Suboptimal Controllers and Communication Range

The analytic properties of the feedback matrix  $K(\lambda)$  have a strong impact on the structure of the optimal control law. By analyzing  $K(\lambda)$  we want to derive some information concerning the possibility of implementing a suboptimal control law, through the truncation of the above series (15). Therefore, it becomes important to determine the decay rate of its coefficients.

This information is related to the location in the complex plane of the singularities of (15). More precisely, the decay rate of the coefficients of (15) corresponding to positive powers of  $z$  is determined by the singularity

$$\lambda_M = \min\{\lambda(K) : |\lambda(K)| > 1\}$$

while for the decay rate of the coefficients corresponding to negative powers of  $z$  we have to consider

$$\lambda_m = \max\{\lambda(K) : |\lambda(K)| < 1\}.$$

From the analytical expression of the matrix  $K(\lambda)$ , it follows that such singularity points are solutions of the equations

$$a(\lambda)^2 + q = 0 \quad (16)$$

and

$$2a(\lambda) + 2\sqrt{a(\lambda)^2 + q} + q = 0, \quad (17)$$

which are equivalent respectively to

$$a(\lambda) \pm i\sqrt{q} = 0, \quad (18)$$

and

$$a(\lambda) + \frac{q}{4} - 1 = 0. \quad (19)$$

Analyzing the expression of  $a(\lambda)$

$$a(\lambda) = -1 + \frac{2d}{(\alpha + \xi_{1,i})^3} - \frac{4\Sigma^6 d}{15(\alpha + \xi_{1,i})^9} + \sum_{\substack{k=-\infty \\ k \neq 0}}^{\infty} a_k e^{-ik\lambda},$$

it is easy to see that, when the number of interacting cantilevers  $N$  is finite, (16) and (17) are reciprocal equations of degree  $N$ , with  $N$  even.

Reciprocal equations with even degree are equations of the form

$$ax^{2k} + bx^{2k-1} + cx^{2k-2} + \dots + rx^k + \dots + cx^2 + bx + a = 0, \quad (20)$$

that can be easily rewritten as

$$a(x^k + x^{-k}) + b(x^{k-1} + x^{-k+1}) + c(x^{k-2} + x^{-k+2}) + \dots + r = 0.$$

Defining  $t := x + x^{-1}$ , it is not difficult to verify that  $t^2 - 2 = x^2 + x^{-2}$ ,  $t^3 - 3t = x^3 + x^{-3}$  and, in general,  $x^m + x^{-m}$  is a polynomial of degree  $m$  in  $t$ . It follows that the reciprocal equation (20) can be rewritten as

an equation of degree  $k$  in the variable  $t$ . Hence, the solution of a reciprocal equation of degree  $2k$  can in general be reduced to solving one polynomial equation of degree  $k$ , as well as at most  $k$  quadratic equations. In what follows, we use this property to reduce the order of the polynomials defining the singularities and find an explicit analytical expressions for them.

We explicitly consider, at first, the case where the dynamics of each cantilever is affected only by the presence of the two closest cantilevers, i.e. the case where in (8) only  $a_1 = a_{-1}$  are different from zero. It follows that, from (16), we obtain four singularity points, which after some algebraic calculations, are given by

$$\lambda_{1,2,3,4} = -\frac{1}{2} \frac{a_0 \pm i\sqrt{q}}{a_1} \pm \frac{1}{2} \sqrt{\left(\frac{a_0 \pm i\sqrt{q}}{a_1}\right)^2 - 4},$$

while from (17) we get

$$\lambda_{5,6} = -\frac{1}{2} \frac{4a_0 + q - 4}{4a_1} \pm \frac{1}{2} \sqrt{\left(\frac{4a_0 + q - 4}{4a_1}\right)^2 - 4},$$

where in both cases  $a_0 = -1 - \frac{2d}{(\alpha + \xi_{1,t})^3} + \frac{4\Sigma^6 d}{15(\alpha + \xi_{1,t})^9}$ .

In the simulations that we performed, we set  $\alpha = 1.2$  and  $\Sigma = 0.03$ . For this value of  $\alpha$  the nonlinear system has three equilibrium points, therefore it can be associated with three linearized systems. Fig (4) shows how the maximum and minimum modulus singularities, respectively  $\lambda_M$  and  $\lambda_m$ , move as  $a_1$  varies in  $[\frac{a_0}{8}, \frac{a_0}{4}]$  for these three systems. As expected, the value of  $\lambda_M$  tends to decrease, while the value of  $\lambda_m$  tends to increase, meaning that the decay rate of the coefficients becomes slower: as the influence of the neighbouring cantilevers becomes stronger, the controller needs more information to stabilize and optimize the performance of the system.

We then considered the case of four interacting cantilevers. The explicit expression for the singularities is, from (16)

$$\lambda_{1,\dots,8} = -\frac{a_1}{4a_2} \pm \frac{\sqrt{a_1^2 - 4a_2(a_0 \pm i\sqrt{q} - 2a_2)}}{4a_2} \\ \pm \frac{1}{2} \sqrt{\left(-\frac{a_1}{2a_2} \pm \frac{\sqrt{a_1^2 - 4a_2(a_0 \pm i\sqrt{q} - 2a_2)}}{2a_2}\right)^2 - 4},$$

and from (17)

$$\lambda_{9,\dots,12} = -\frac{a_1}{4a_2} \pm \frac{\sqrt{a_1^2 - a_2(4a_0 + q - 4 - 8a_2)}}{4a_2} \\ \pm \frac{1}{2} \sqrt{\left(-\frac{a_1}{2a_2} \pm \frac{\sqrt{a_1^2 - a_2(4a_0 + q - 4 - 8a_2)}}{2a_2}\right)^2 - 4}.$$

Simulations show that the decay rate of the coefficients of  $K$  is slower as in Fig (4).

## 5 Conclusion

The new techniques of optimal control of spatially invariant systems were used to design optimal controllers for an array of microcantilevers that is used to increase throughput in atomic force microscopy. Analytical formulae were obtained for the optimal controller, which were then used to design suboptimal controllers with limited communication from the sensors. The use of the spatial invariance properties of the system was crucial in developing finite dimensional controllers.

## References

- [1] M. Ashhab, M. Salapaka, M. Dahleh, and I. Mezić, "Control of Chaos in Atomic Force Microscopes," *Proceedings of the American Control Conference*, Albuquerque, New Mexico, pp. 196-202, June, 1997.
- [2] M. Ashhab, M. Salapaka, M. Dahleh and I. Mezić, "Melnikov-based Dynamical Analysis of Microcantilevers in Scanning Probe Microscopy", *UCSB Technical Report*, 1997.
- [3] E.W. Kamen, "Stabilization of Linear Spatially-Distributed Continuous-Time and Discrete-Time Systems", in *Multidimensional Systems Theory*, Chap.4. N.K. Bose (ed.). D. Reidel Publishing Company, 1985.
- [4] B. Bamieh, F. Paganini and M.A. Dahleh, "Optimal Control of Distributed Actuator and Sensor Arrays", to appear in *Proc. SPIE 5'th Ann. Intl. Symp. on Smart Structures and Materials*, San Diego, March 1998.
- [5] B. Bamieh, "The Structure of Optimal Controllers of Spatially-Invariant Distributed Parameter Systems", in *Proc. 36'th IEEE Conference on Decision and Control*, San Diego, CA, December, 1997.
- [6] B. Bamieh, F. Paganini and M.A. Dahleh, "Distributed Control of Spatially Invariant Systems", submitted to the *IEEE Trans. Automatic Control*, May 1998.
- [7] G. Binnig, C.F. Quate, and C. Gerber. Atomic force microscope. *Physical Review Letters*, 56, no.9:pp. 930-3., 1986.
- [8] Dror Sarid, *Scanning Force Microscopy*, Oxford University Press, New York, 1994.
- [9] Jacob N. Israelachvili, *Intermolecular and Surface Forces*, Academic Press, 1985.
- [10] S. C. Minne, S. R. Manalis, and C. F. Quate, "Parallel atomic force microscopy using cantilevers with integrated piezoresistive sensors and integrated piezoelectric actuators," *Appl. Phys. Lett.*, 67 (25), 3918-3920, December, 1995.
- [11] S. C. Minne, S. R. Manalis, A. Atalar, and C. F. Quate, "Independent parallel lithography using the

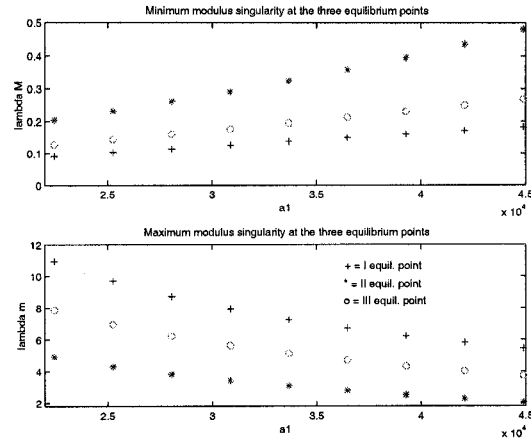


Figure 2: Variation of the minimum and maximum modulus singularities.

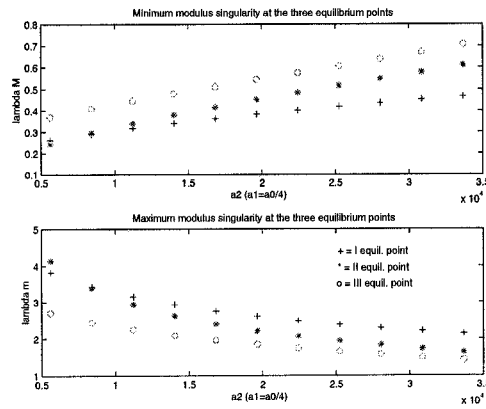


Figure 3: Variation of the minimum and maximum modulus singularities.

atomic force microscope," *J. Vac. Sci. Technology*, B, 14(4), 2456-2461, July, 1996.